Rehm. 2003. Poster # 926; Presented at the 9th International Conference on Functional Mapping of the Human Brain, June 19-22, 2003, New York, NY. Abstract available on CD-Rom in Neuroimage, Vol. 19, No 2.

Inter-subject Spatial Registration of the Human Cerebellum

Kelly Rehm [1], Jon Anderson [2], Roger Woods [3], David Rottenberg [1,2]

Departments of [1]Radiology and [2] Neurology, University of Minnesota, Minneapolis, U.S.A and [3] Department of Radiology, UCLA, Los Angeles, U.S.A.

www.neurovia.umn.edu/incweb

ABSTRACT

We and others have discussed data analysis benefits that may accrue from registering the cerebellum and the cerebrum independently [1]. In this work we investigated several methods for computing intersubject cerebellar registration. We compared linear transformation methods, block-resampling, and nonlinear (warping) approaches for registering high-resolution T1-weighted MR volumes with respect to landmark localization and intensity characteristics. For comparison, we included two alignment transformations computed using the whole brain but applied only to the cerebellum.

MOTIVATION

Intersubject registration of our fMRI static force dataset [2] was performed using a 7th-order polynomial warp transformation (AIR, Woods [3]). Warp order selection was made on the basis of the functional results (Strother, personal communication). Figure 1 depicts mid-sagittal cerebellar slices from each of the 16 co-registered subjects and the corresponding slice from the template volume. Fissure locations were marked on the template slice according to Schmahmann [4] and plotted on the subjects' slices. After intersubject registration there was considerable variability in the location of the primary fissure relative to its template location.

Figure 1. Mid-sagittal slice of 16 subjects aligned with 7th-order AIR5.03; the template slice is at lower right. Fissures are colored as follows: pink, precentral; green, preculminate; red, primary (arrow); cyan, superior posterior; yellow, prepyramidal/prebiventer; blue, secondary; gold, posterolateral.

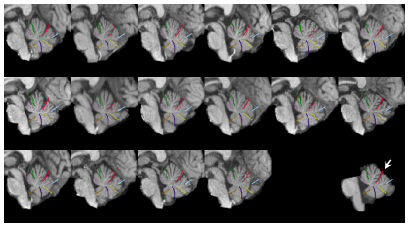

METHODS

MRI volumes and spatial compartments

Sixteen T1-weighted MRI scans of normal subjects were acquired during an fMRI experiment using a static force protocol [2]. Voxel dimensions were 0.86 x 0.86 x 1.0 mm. The Montreal Neurological Institute 27-scan-average T1 MRI volume [5] served as our template and was manually stripped and divided into spatial compartments, including the cerebellum and brainstem below the inferior colliculi.

Figure 2. Axial, coronal and sagittal slices through the template brainstem and cerebellum.

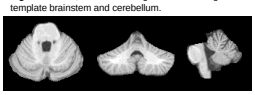

The cerebellum-brainstem compartment was generated for each subject by computing a warp transformation of the template volume onto the subject volume. A transformation of the template compartment mask served as the initial subject compartment, which was then automatically adjusted according to local intensity characteristics. The resulting compartment boundaries were reviewed and manually adjusted to produce a smooth mask.

Registration methods

Grodd. Rigid-body translation and rotation to a pose in which the floor and apex of the fourth ventricle define three orthogonal planes; a 12-part piecewise-linear scaling was then applied based on the lateralmost points of the cerebellar hemispheres, the anteriormost point of the pons, the dorsal extent of the cerebellar hemispheres, the superiormost point of the vermis, the inferior extent of the hemispheres, and the inferiormost point of the vermis ([1], see Figure 3).

VA pose. Rigid-body translation and rotation to a standard pose in which the posterior commissure, obex and apex of the fourth ventricle define three orthogonal planes [6].

VA Spose. Includes12-part scaling using Grodd's method (Figure 4.)

Figure 3. Triangle defining Grodd's pose and the resulting bounding box (white) and rostral-caudal and anterior-posterior axes (green). The red line passes through the caudal point of the vermis.

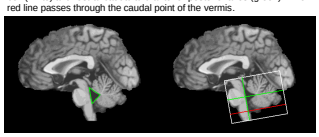

Figure 4. Triangle defining VA pose and the resulting bounding box (white) and rostral-caudal and anterior-posterior axes (green). The red line passes through the caudal point of the vermis.

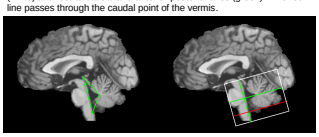

BRIU12. Block application of 12-parameter affine transforms [7]. This algorithm aligns two volumes using a 12-parameter affine transformation and a ratio-image cost function (after the method used in AIR) and then resamples the subject volume to match the template volume. Next, the template and transformed subject volumes are bisected in each dimension to form 8 blocks, and a transform is computed for each block. The subject volume is resampled again using the alignment information from the whole brain and the block transformations. The process is repeated until a minimum block size is reached (e.g., 2.5 cm^3), and continuity is enforced by overlapping blocks; each new coordinate is a weighted average of the coordinates computed for its neighborhood of overlapping blocks.

AIR5.03 Polynomial warp transformations (orders 2-7) [3]. The mask used in computing warp transformations was spatially dilated at the cerebellum-occipital lobe boundary to ensure a smooth surface.

Landmarks

Cerebellar landmarks were selected for the template and each subject based on the Schmahmann atlas [4]:

- apex of V4 ***{V4}***
- tip of the lingula ***{L}***
- floor of the primary fissure (midline) ***{Pf}***
- tip of the nodulus ***{N}***
- floor of the preculminate fissure (midline) ***{Pc}***
- floor of the prepyramidal fissure (midline) ***{Py}***
- floor of the secondary fissure (midline) ***{Sf}***

No off-midline landmarks could be reliably identified.

Evaluation

Alignment quality was assessed using the following metrics:

- landmark cluster raidus
- landmark displacement vs. template landmark position
- volume of intersection of aligned subjects
- correlation of group average volume and template intensities
- subject-subject pairwise intensity correlations
- subject-template intensity correlations

A landmark's cluster radius was defined as the standard deviation of the distances of each subject's landmark from the mean position. Landmark displacement was the Euclidian distance of the mean position from the corresponding template position.

RESULTS

A group average volume was computed from the 16 subjects using each registration method and trilinear interpolation. Figures 5 and 6 illustrate slices through the group volumes for the planes in Figure 2.

Naming conventions:

AIR^{WN} refers to whole-brain, Nth order polynomial AIR warp.
BRIU12^{C} refers to cerebellum-only, block resampling.

Although Woods advises caution in using high-order polynomial warps to align volumes with limited fields of view [8], for this investigation we computed cerebellar alignments up to the same order employed for whole-brain alignment.

Figure 5. Axial, coronal and sagittal slices through group volumes produced using, from left to right (columns): AIR^{W7}, BRIU12^{W}, VA pose, Grodd, VA Spose, BRIU12^{C}.

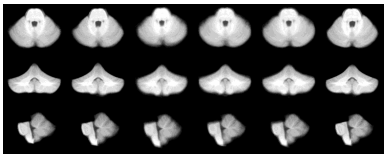

Figure 6. Axial, coronal and sagittal slices through group volumes produced using, from left to right (columns): AIR^{C2}, AIR^{C3}, AIR^{C4}, AIR^{C5}, AIR^{C6}, Air^{C7}. Arcs indicate rostral vermis.

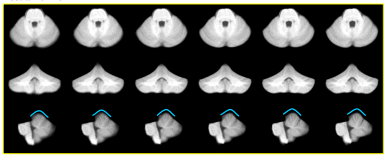

Landmark positions after alignment (Table 1) were calculated directly for VA pose, VA Spose and Grodd's method, whereas a mark volume was computed for the remaining methods using the registration transform, and the centroid of each mark was treated as the new landmark position.

Volume and correlation metrics (Table 2) were computed only on those voxels common to all sixteen subjects after transformation.

Table 1. Landmark metrics: (cluster radius, cluster displacement from template location in millimeters). Entries marked in brown denote minimum values.

Method	*V4*	*L*	*Pf*	*N*	*Pc*	*Py*	*Sf*	Averages
AIR^{W7}	0.6, 2.1	**0.5**, 1.3	**0.7**, 1.7	1.0, 1.8	**1.1**, 2.1	1.2, **0.7**	1.1, 2.0	0.9, 1.7
BRIU12^{W}	0.6, 1.9	0.6, 1.0	1.1, 1.6	1.0, 2.1	1.2, 1.7	0.8, 0.8	0.9, **1.5**	0.9, **1.5**
VA pose	1.0, 4.2	1.0, 2.6	1.4, 3.0	1.1, 3.2	1.4, 4.1	1.1, 2.5	1.2, 3.3	1.2, 3.3
Grodd	0.7, 2.9	1.0, 1.7	0.9, 1.6	**0.7**, 2.4	1.3, 2.6	0.8, **0.7**	0.9, 2.2	0.9, 2.0
VA Spose	0.9, 2.6	0.8, 1.7	1.1, **0.9**	0.9, 2.3	1.2, 2.6	0.8, **0.7**	1.0, 2.2	1.0, 1.9
BRIU12^{C}	**0.5**, 1.6	**0.5**, 1.1	1.1, 1.5	1.0, 2.0	**1.1**, **1.3**	**0.7**, 1.7	1.0, 2.2	**0.8**, 1.6
AIR^{C2}	0.9, 1.1	0.6, 1.9	1.0, 1.4	1.1, **1.5**	**1.1**, 2.0	1.2, 1.4	1.0, 2.7	1.0, 1.7
AIR^{C3}	**0.5**, 1.1	0.6, 2.1	0.9, 1.5	0.9, **1.5**	**1.1**, 2.2	1.4, 2.5	1.3, 3.4	1.0, 2.0
AIR^{C4}	0.6, 1.8	0.7, 1.2	1.0, 1.6	1.0, 1.6	1.2, 1.5	1.5, 2.5	1.5, 2.8	1.1, 1.8
AIR^{C5}	0.6, 1.8	**0.5**, 1.2	1.2, 1.2	0.9, 1.7	**1.1**, 1.8	1.3, 1.8	1.3, 2.3	1.0, 1.7
AIR^{C6}	**0.5**, 1.4	**0.5**, 1.0	1.2, 1.7	0.9, 1.7	1.2, 1.5	1.3, 1.8	0.9, 2.2	0.9, 1.6
AIR^{C7}	0.6, **0.8**	**0.5**, **0.7**	1.0, 2.4	1.0, 1.6	**1.1**, 1.4	1.0, 2.8	**0.8**, 2.9	0.9, 1.8

Table 2. Volume and intensity metrics. Entries marked in brown denote maximum values.

Method	Intersection volume (cm^3)	Group- template correlation R	Subject-subject correlation R	Subject-template correlation R
AIR^{W7}	181.2	0.77	0.74	0.71
BRIU12^{W}	183.1	0.76	0.72	0.70
VA pose	142.9	0.58	0.54	0.46
Grodd	153.0	0.66	0.55	0.52
VA Spose	156.3	0.66	0.57	0.54
BRIU12^{C}	191.7	0.78	0.75	0.72
AIR^{C2}	181.3	0.74	0.71	0.67
AIR^{C3}	186.5	0.77	0.74	0.71
AIR^{C4}	192.0	0.81	0.76	0.74
AIR^{C5}	**194.0**	0.82	0.77	0.76
AIR^{C6}	193.6	0.84	0.78	0.77
AIR^{C7}	189.4	**0.86**	**0.79**	**0.79**

Template volume = 206.5 cm^3. Ten of the subject volumes were smaller than the template.

DISCUSSION

The group-average slices exhibit increased clarity with an increase in the sophistication of the alignment method. In the high-order-warp group volumes (Fig. 6, AIR$^{C5\text{-}C7}$) the rostral vermis (arcs) and primary fissure were particularly well-resolved in the sagittal views.

Whole-brain alignment methods (AIR^{W7}, BRIU12^{W}) and all cerebellum-specific alignment methods with the exception of the simple VA pose resulted in landmark cluster radii of approximately one voxel and cluster displacements of 2 voxels or less (Table 1). BRIU12 calculated on the cerebellar compartment produced the minimum landmark cluster size but not the minimum displacement. The perceived differences in clarity of the group-average slices (Figs. 5 and 6) were not reflected by the landmark metrics.

Volume metrics appeared to capture the visible effects of increasingly sophisticated alignment methods. The simple methods that have blurry group-average slices (Fig. 5) were characterized by low intersection volumes and poor correlations (see Table 2). BRIU12^{C} and AIR$^{C2\text{-}C7}$ had intersection volumes approaching that of the template volume. This metric suggests that alignment improves up to AIR^{C5} and then worsens; intensity correlations appear to indicate an improvement in alignment up to AIR^{C7}.

Neither these evaluation metrics nor visualization of group-average slices was sufficient to identify cases in which subjects' aligned volumes were visibly distorted.

Polynomial warps as implemented in AIR are known to be sensitive to masks and limited fields of view. [Online documentation by Woods indicates that order 4 and higher "can lead to unexpected or even bizarre results".] In Figure 7 subject volumes have been rotated and translated to match the orientation of the template volume. When mid-sagittal slices of the reoriented volumes are compared to the mid-sagittal AIR^{C7} slices in Figure 8, the rostral vermis appears deformed in several instances (arrows in Fig. 8).

Figure 7. Sagittal slices in same orientation as the template slice at lower right.

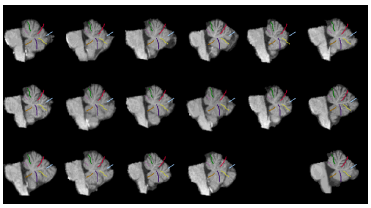

Figure 8. Sagittal slices prepared using AIR^{C7}. Template slice is at lower right. Arrows indicate dubious results.

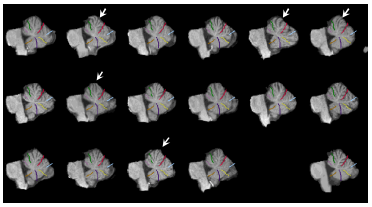

Fifth and higher-order warps computed with the field of view limited to the cerebellar compartment proved to be unstable. In contrast, block-resampling using a 12-parameter affine transformation (which produced a high intersection volume and the minimum landmark cluster size for this group of subjects), produced visually plausible transformed volumes (Figure 9). Localization of the primary and prepyramidal fissures in the midline is greatly improved over the whole-brain approach illustrated in Figure 1.

Figure 9. Sagittal slices prepared using BRIU12^{C}. Primary fissure, red (arrow); prepyramidal/prebiventer fissure, yellow (arrowhead).

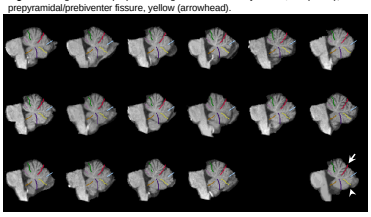

CONCLUSIONS

For intersubject registration of T1-weighted MRI scans of normal subjects one can improve structural alignment by treating the cerebellum as a separate compartment. Non-linear registration is preferable to piecewise linear scaling, but high-order polynomial warps should be used with caution. Although quantitative metrics may be indicative of "goodness of registration", visual inspection of co-registered volumes is necessary in order to select the most successful approach for a given group of subjects.

REFERENCES

1. Grodd W, *et al. Human Brain Mapping* 13:55-73,2001.
2. Muley, *et al. NeuroImage*. 13:185-195.
3. Woods RP, *et al. Journal of Computer Assisted Tomography* 22:153-165, 1998
4. Schmahmann JD, *et al. MRI Atlas of the Human Cerebellum*. Academic Press, San Diego, 2000.
5. Holmes CJ, *et al. NeuroImage*. 3(3):S28, 1996.
6. Rehm K, *et al. NeuroImage*. 11(5):S536, 2000.
7. Anderson JR, personal communication.
8. Woods RP. Online documentation for AIR5.03 program *align_warp*: www.bishopw.loni.edu/AIR5/index.html

This work was supported in part by NIH grant P20 MH57180.